HETEROCYCLES, Vol. 104, No. 7, 2022, pp. 1191 - 1211. © 2022 The Japan Institute of Heterocyclic Chemistry
Received, 15th February, 2022, Accepted, 15th April, 2022, Published online, 22nd April, 2022
DOI: 10.3987/COM-22-14641

SYNTHESIS AND OPTICAL PROPERTIES OF SUBSTITUTED 5,6,7,8-TETRAAZA-AZULENO[1,8-*b*,*c*]FLUORENES, SMALL ORGANIC MOLECULES OF UNUSUAL TOPOLOGY DESIGNED FOR CIRCULARLY POLARIZED LUMINESCENCE

Tadeusz Lemek,[a]* Krzysztof Danel,[b] Oskar Michalski,[b] and Wojciech Nitek[c]

a) Tadeusz Lemek; R&D Institute of Celon Pharma S.A., ul. Marymoncka 15, 05-152 Kazuń Nowy, Poland; E-mail: Tadeusz.Lemek@celonpharma.com; b) Krzysztof Danel, Oskar Michalski; Institute of Chemistry, Faculty of Food Technology, University of Agricultural in Cracow; ul. Balicka 122, 30-149 Cracow, Poland; E-mail: Krzysztof.Danel@urk.edu.pl; Oskar.Michalski@urk.edu.pl. c) Wojciech Nitek; Department of Chemistry, Jagiellonian University of Cracow; ul. Gronostajowa 12, 30-387 Cracow, Poland; E-mail: Wojciech.Nitek@uj.edu.pl

Dedicated to Professor Herbert Mayr on the occasion of his 75th birthday

Abstract – Helical photoluminescent substituted 5,6,7,8-tetraaza-azuleno[1,8-*b*,*c*]fluorenes were obtained as racemates. The compounds have been designed for circularly polarized luminescence. Some of the compounds were separated on to enantiomers with chiral HPLC column and showed Cottons effects in absorption and emission spectra. The experimental results were compared with DFT calculations, which led us to assess the chirality to structure.

INTRODUCTION

Circularly polarized light (CPL) is of great importance in science and photonic technologies.[1] There are two main methods to generate a polarized light output from OLED, either from chiral polymers being the active layer or via a chiral small-molecule dopant.[2] Recently the 4f-based metal complexes with strong CPL emission have been recognized as candidates for potential technological applications. However the difficulties with obtaining of highly pure samples and significant production costs stunt progress in this case.[3] Thus chiral luminescence organic molecules are essential for development in advance photonic technology. In comparison to a plethora of available OLED candidates,[4] the number of the circularly

polarized light emitting compounds, thermally and chemically stable, is still not outstanding. In former works we described the synthesis and spectral properties of azafluoranthene and heteroazulene derivatives.[5] Specially, the second group of compounds has focused our attention, as they contained helical arrangements of four *ortho*-fused rings. Their helicity is the result of steric repulsion between hydrogen atoms in "fiord" regions as well as the demanding geometry imposed by the seven-membered ring embedded in the main framework of the molecules. Additionally, conjugated polycyclic hydrocarbons containing seven-membered rings have been rarely explored, this has prompted us to focus our effort on the synthesis of azulenefluorene-like helical structures. It worth to admit, merging of seven-member rings in terms of the application of carbon materials to organic electronics, may become a key factor.[6] The advantage of being intrinsically helical and the choice between their right-handed and left-handed enantiomeric forms, make azahelicenes attractive candidates in CPL technology. To fulfil the criteria of satisfying operational parameters must be considered sufficient high racemisation barrier when designing the active molecule. Our earlier findings delivered helicenes of a low racemisation barrier,[7] thus excluding them from the construction of CPL emitting devices. Therefore we decided to hinder the quick inversion of enantiomers either by introducing an additional fused ring or a bulky group. In this study we describe the synthesis of racemic mixtures and their separation on to enantiomers, as well as the optical properties of novel heterocycles - substituted 5,6,7,8-tetraaza-azuleno[1,8-*b*,*c*]fluorenes, helical compounds – of unusual topology. The precursors are derived from substituted pyrazolo[3,4-*b*]pyridines. The idea is that an aryne generated during elimination/addition reaction of halogens attack the intramolecular neighbouring ring to form aza[5 or higher]helicenes. In this study we present preliminary results in helical tetraaza-azulenofluorenes investigations and, have focused our attention on α-carbolins as the starting compounds, which were obtained in a one-pot, three component cascade reaction.[8]

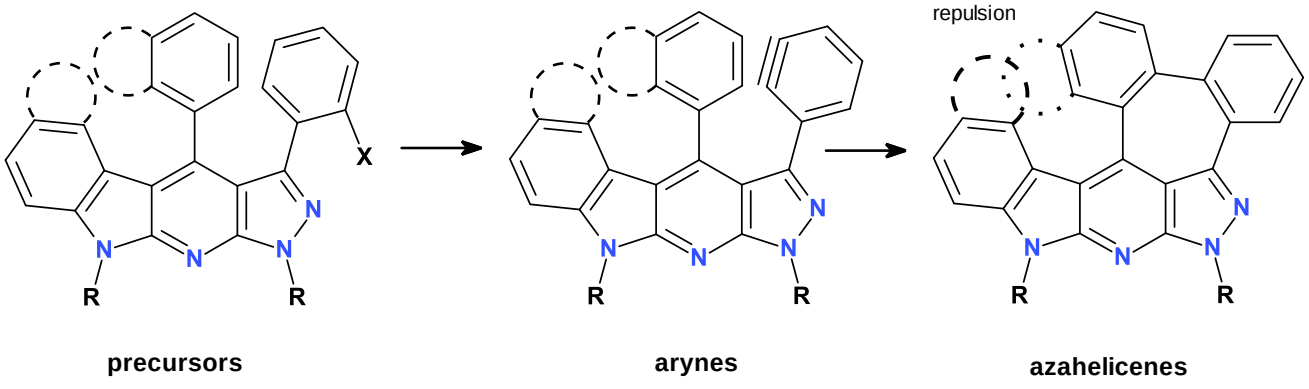

RESULTS AND DISCUSSION

The *α*-carbolines **1-5** with the structures drawn below as precursors for the synthesis of tetraaza-azulenefluorenes **1a-5a**, were obtained in a one-pot, three component cascade reaction from appropriate substituted indolinone, arylaldehyde and 5-(2-chlorophenyl)-2-phenylpyrazol-3-amine in ionic liquid Br [Bmim] as the solvent and *para*-toluenesulfonic acid as catalyst at 140 ºC, as described by Bazgir *et al*.[8] Many examples of application of this reaction in more multicomponent variations can be found in ref 8b. (see also Supp. Inf. for more details)

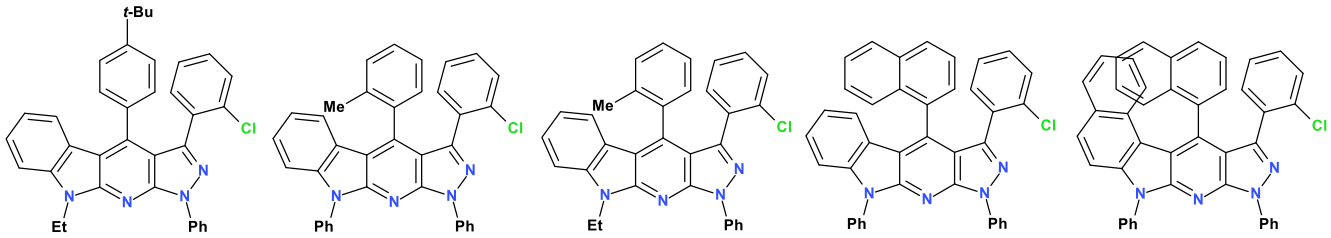

1 **2** **3** **4** **5**

Thus, the compound **1a** (*M*)(*P*)(±)-15-*tert*-butyl-8-ethyl-6,8-dihydro-6-phenyl-5,6,7,8-tetraazadibenzo[4,5:6,7]azuleno[1,8-*b*,*c*]fluorene obtained from the precursor **1** (Scheme 1) does not show diastereotopic differentiation at CH_2 protons of the ethyl group in ^{1}H-NMR spectrum. The compound shows absorption in UV-Vis spectrum at λ_{max} = 389 nm and emission (PL) at λ_{max} = 482 nm (Figure 1).

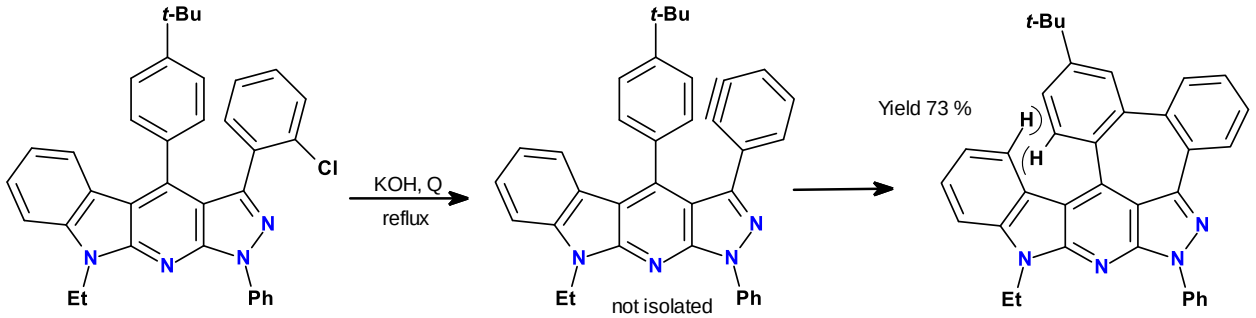

1 **1a**

Scheme 1. Synthesis of (*M*)(*P*)(±)-15-*tert*-butyl-8-ethyl-6,8-dihydro-6-phenyl-5,6,7,8-tetraazadibenzo[4,5:6,7]azuleno[1,8-*b*,*c*]fluorene

Calculated UV-Vis spectrum gave absorption maxima at λ_{max} = 425 nm and λ_{max} = 347 nm, and correspondingly, PL at λ_{max} = 526 nm. The racemic mixture could be possibly separated on two fractions (Figure 2) with HPLC OD-H chiral column with approximated ratio 1:1, but the fractions devoid of optical rotation measured next day. We assume that this compound posses a low racemisation barrier and racemised after resolution overnight. That was consecutively confirmed by the calculated racemisation barrier value of ΔG 6-31G(d) at 298.15 K 99.0 kJ/mol, and half-life time (calculated time after which the

mixture contains both enantiomers in 3:1 ratio) at 298.15 K is 207 minutes, which explains the disappearance of the optical activity of **1a**. Calculated specific optical rotation for enantiomer (*M*) $[\alpha]_D$ = -170º suggests the configuration (*M*)(-) and (*P*)(+) for enantiomers of **1a**. Calculations were carried out with the GAUSSIAN 09W rev. A.02 program for M enantiomers. Preliminary geometry optimizations were done semiempirically at AM1 level. Final structure optimizations were accomplished with the use of DFT B3LYP functional and 6-31G(d) basis set including the polarisable continuum model (PCM) for modelling molecules in solution (CH_2Cl_2), (for more details see Supp. Inf.).

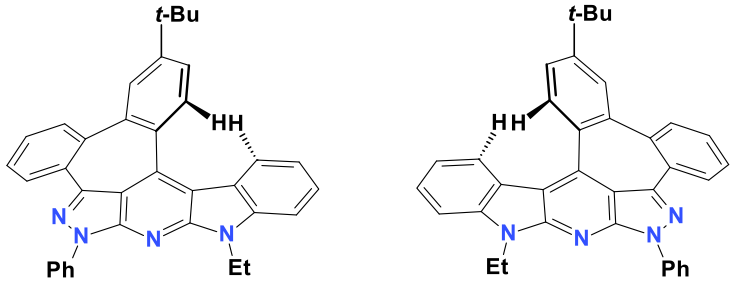

1a (*M*)(-) Enantiomer **1a** (*P*)(+) Enantiomer

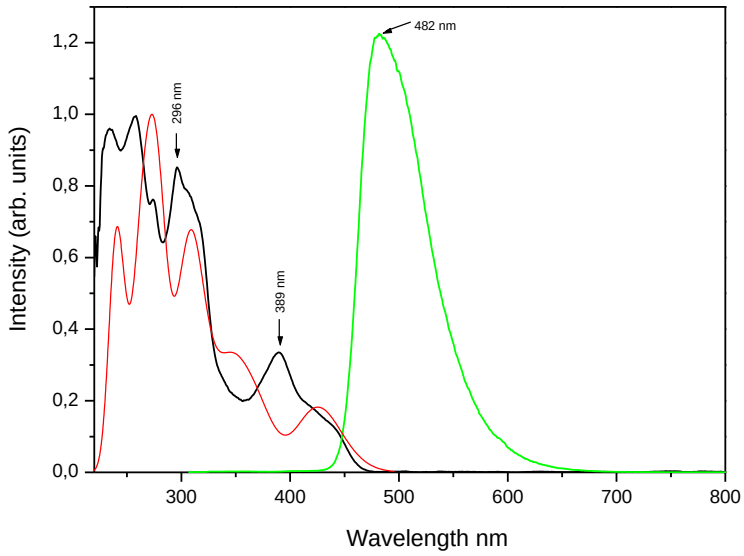

Figure 1. UV absorption (black line), calculated absorption spectrum (red line) and emission spectrum (green line) of **1a**, in CH_2Cl_2. Excitation at 296 nm

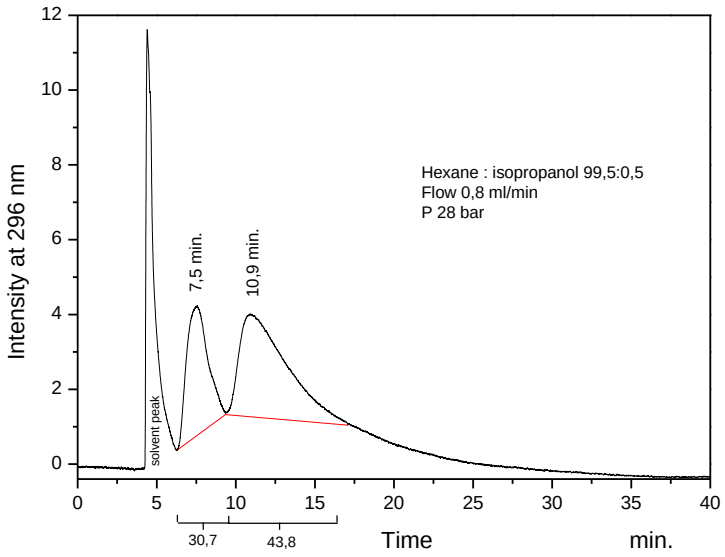

Figure 2. Separation of **1a** on to enantiomers on HPLC ODH column with hexane-isopropanol eluent

Next compound with the methyl group at the sterically crowded position 13 is (*M*)(*P*)(±)-6,8-dihydro-13-methyl-6,8-diphenyl-5,6,7,8-tetraazadibenzo[4,5:6,7]azuleno[1,8-*b*,*c*]fluorene **2a** (Scheme 2).

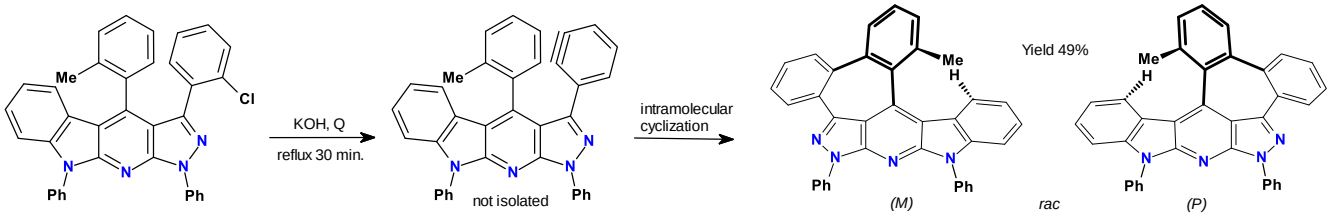

2 **2a**

Scheme 2. Synthesis of (*M*)(*P*)(±)-6,8-dihydro-13-methyl-6,8-diphenyl-5,6,7,8-tetraazadi-benzo[4,5:6,7]azuleno[1,8-*b*,*c*]fluorene

For three compounds **2a**, **3a** and **4a** it was possible to obtain single crystals suitable to X-ray diffraction data collection. Compound **2a** crystalize in $P2_1/c$ space group. Uneven and helically twisted molecules of them preclude the regular π–π stacking, however numerous interactions with π electron systems are observed in the crystal structure (Figure 3). Three of the them should be mentioned as the interactions which significantly determines the crystal packing. Atoms N1 - C16 which forms approximately flat system of four aromatic rings in central part of molecule, interacts with their counterparts in molecule related by inversion located at (1/2, 1/2, 1/2). This π–π interaction, with 3.468 Å distance between planes

forms a kind of dimers of (*P*) and (*M*) enantiomers. Hydrogen atom joined to atom C41 is in the 2.943 Å distance to centre of phenyl ring formed by atoms C35 - C40 related also by inversion, but in position (0, 1/2, 1/2). Geometry of this interaction indicates the C-H - π interaction type III.[9] These pair of symmetry related C-H - π interactions are joining mentioned above π–π dimers in supramolecular chain along direction [0 1 0] in lattice (Figure 3). "The "edge to face" interaction between phenyl rings formed by atoms C23 - C28 and C29 - C34 transformed by gliding mirror plane located at (x, 1/4, z), is also noticeable. This contact is responsible for bindings between mentioned chains perpendicularly to their axes.

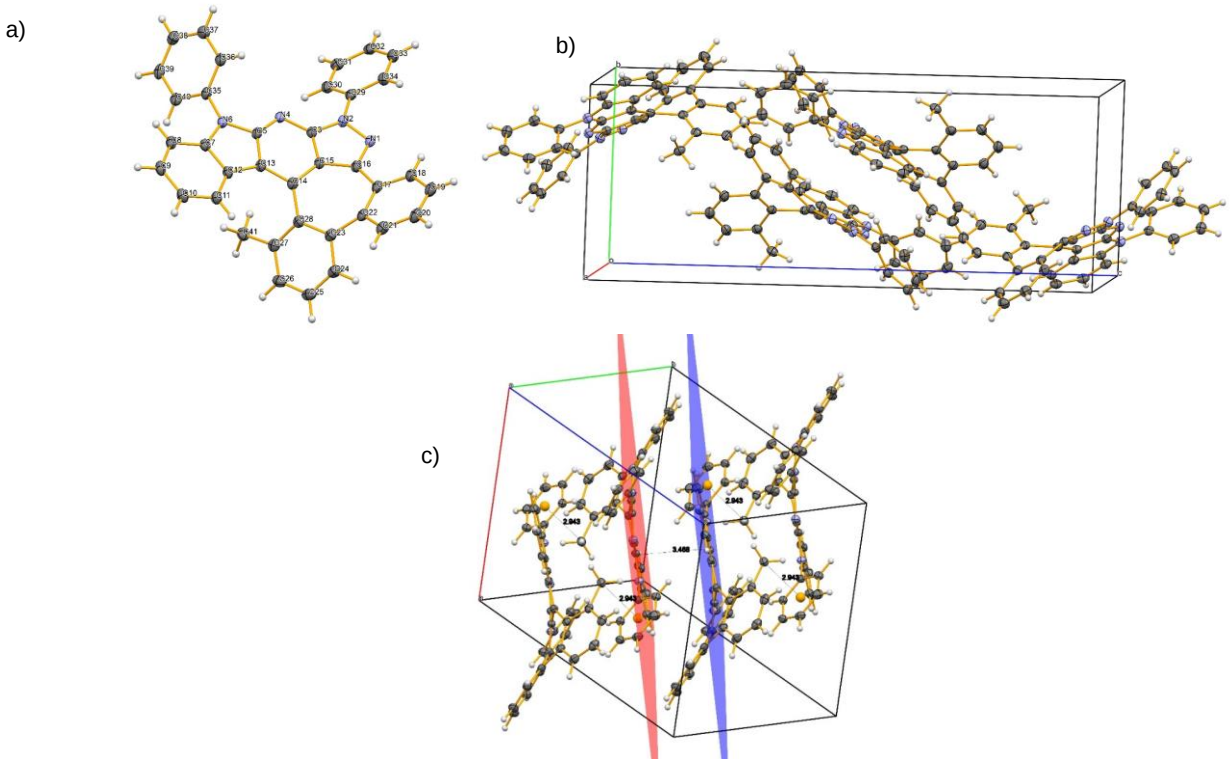

Figure 3. X-Ray structure of the compound **2a**: a) single molecule; b) crystal packing approximately towards [1 0 0] direction; c) π–π and C-H – π interactions

Compound **2a** shows absorption in UV-Vis spectrum at λ_{max} = 388 nm and emission peak (PL) at λ_{max} = 479 nm (Figure 4). Calculated UV-Vis spectrum shows absorption maxima at λ_{max} = 422 nm and λ_{max} = 350 nm. The racemic mixture can be separated on two fractions (Figure 5) on OD-H chiral column with hexane-isopropanol eluent. The CD-spectrum of the first fraction (retention time 15.6 min.) shows weak positive Cottons effect with λ_{max} = 320 nm, and stronger negative at λ_{max} = 290 nm (Figure 6). Comparison with calculated CD-spectra and measured specific optical rotation $[\alpha]_D^{20}$ = +869º (± 143º) (CH_2Cl_2) leads to assessment the configuration for the first fraction compound as (*M*)(+)-6,8-dihydro-

13-methyl-6,8-diphenyl-5,6,7,8-tetraazadibenzo[4,5:6,7]azuleno[1,8-*bc*]fluorene. Calculated specific optical rotation for enantiomer (*M*) $[\alpha]_D$ = + 150º confirms the configuration (*M*)(+) for this enantiomer of compound **2a**. The second fraction from HPLC (retention time 25.4 min.) shows opposite effect, week negative Cottons effect with λ_{max} = 320 nm, and stronger positive at λ_{max} = 290 nm (Figure 1 in Supp. Inf.) and the measured optical rotation $[\alpha]_D^{20}$ = -926º (± 187º) (CH_2Cl_2) confirms the configuration (*P*)(-) for this enantiomer of the compound **2a**. Comparison of the measured CD spectra for both fraction from chiral HPLC column shows exact opposite Cottons effects as expected for separated enantiomers of **2a** (Figure 7). Calculated racemisation barrier ΔG 6-31G(d) at 298.15 K is 157 kJ/mol, and half-life time at 298.15 K is longer than 5 400 000 years, what excludes quick racemisation of the **2a** enantiomers. Fluorescence detected circular dichroism (FDCD spectrum) of **2a** fraction (15.6 min.) (*M*)(+)-6,8-dihydro-13-methyl-6,8-diphenyl-5,6,7,8-tetraazadibenzo[4,5:6,7]azuleno[1,8-*b,c*]fluorene shows weak positive Cottons effect at 325 nm and strong negative Cottons effect at 290 nm (Figure 2 in Supp. Inf.). FDCD spectrum of **2a** fraction with retention time 25.4 min. (*P*)(-)-6,8-Dihydro-13-methyl-6,8-diphenyl-5,6,7,8-tetraazadibenzo[4,5:6,7]azuleno[1,8-*b,c*]fluorene shows weak negative Cottons effects at 325 nm and strong positive Cottons at 290 nm (Figure 3 in Supp. Inf.). Comparison of both enantiomers FDCD spectra with mirror Cottons effects shows Figure 8.

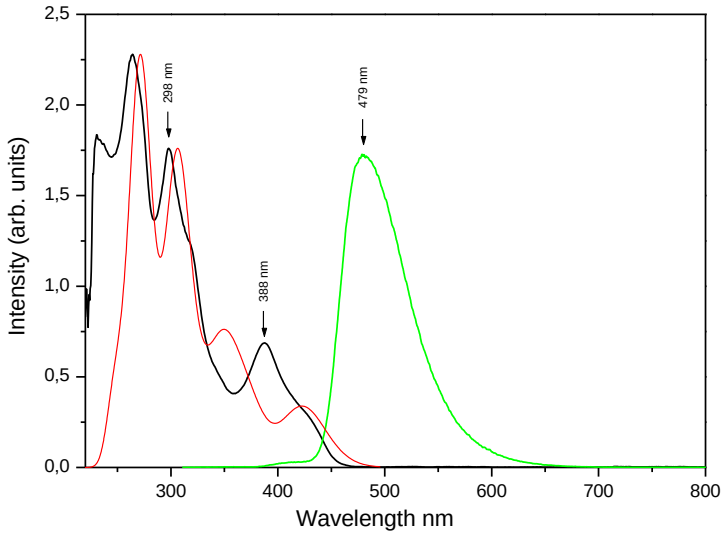

Figure 4. UV absorption (black line), calculated absorption spectrum (red line) and emission spectrum (green line) of **2a** in CH_2Cl_2. Excitation at 298 nm

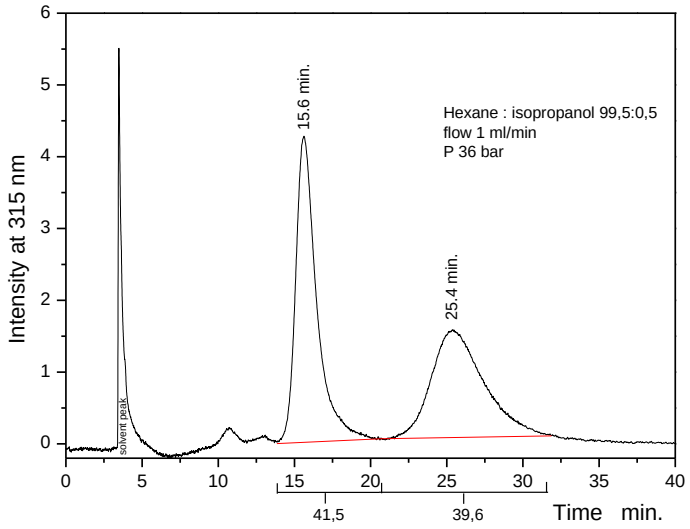

Figure 5. Separation of **2a** on to enantiomers on HPLC OD-H column with hexane-isopropanol eluent

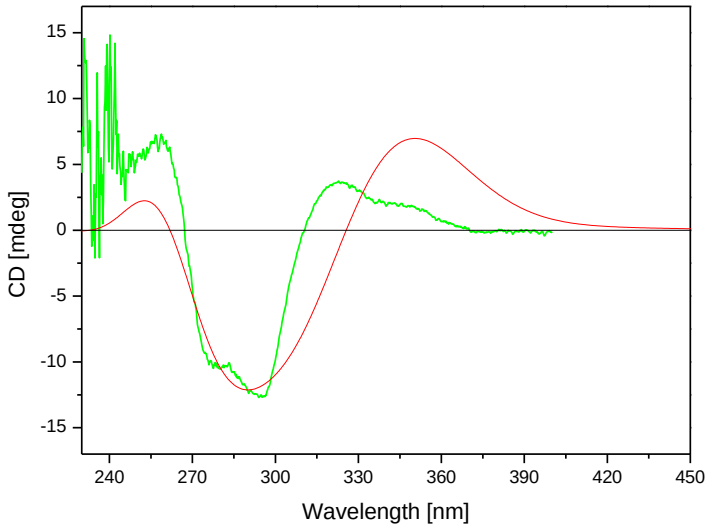

Figure 6. Comparison of the measured CD spectrum of (*M*)(+)-6,8-dihydro-13-methyl-6,8-diphenyl-5,6,7,8-tetraazadibenzo[4,5:6,7]azuleno[1,8-*b*,*c*]fluorene **2a** (green line, CH_2Cl_2) - the first fraction from HPLC with retention time 15.6 min with calculated CD-spectrum (red line), measured specific optical rotation $[\alpha]_D^{20}$ = +869º (± 143º) (CH_2Cl_2)

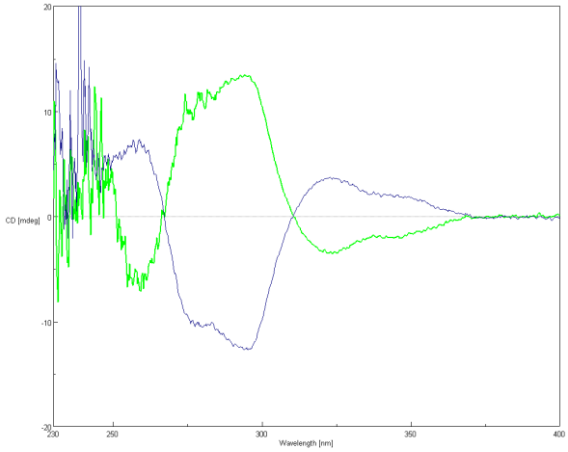

Figure 7. Comparison of the measured CD spectra for separated fractions of **2a**. The first fraction from HPLC 15,6 min. (blue line) **(*M*)(+)-2a**, and second fraction 25,4 min. (green line) **(*P*)(-)-2a**, (CH_2Cl_2).

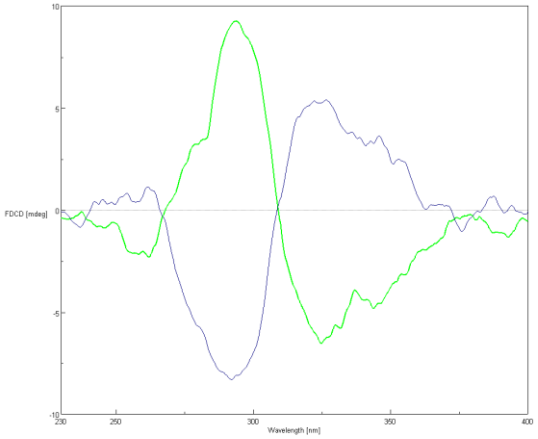

Figure 8. Comparison of the measured fluorescence detected circular dichroism (FDCD spectra) of **2a** enantiomers. **(*M*)(+)-2a** (blue line) and **(*P*)(-)-2a** (green line) (solvent CH_2Cl_2).

Compound **3a** with methyl group at the sterically crowded position 13 and ethyl group with diastereotopic CH_2 protons at the nitrogen in position 8 (Scheme 3).

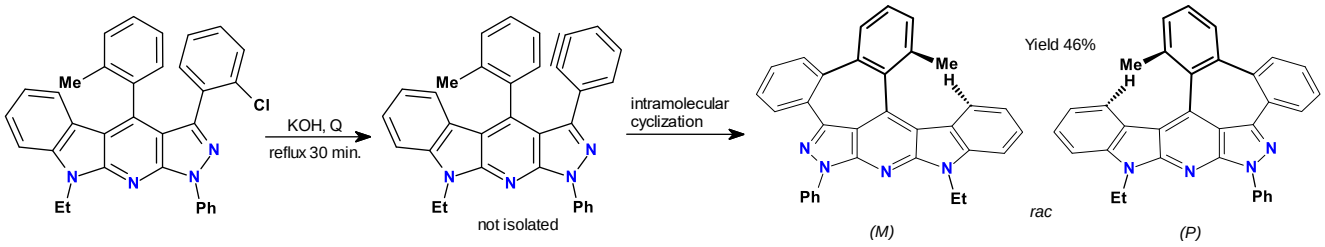

3 **3a**

Scheme 3. Synthesis of (*M*)(*P*)(±)-8-ethyl-6,8-dihydro-13-methyl-6-phenyl-5,6,7,8-tetraazadibenzo[4,5:6,7]azuleno[1,8-*bc*]fluorene

(*M*)(*P*)(±)-8-Ethyl-6,8-dihydro-13-methyl-6-phenyl-5,6,7,8-tetraazadibenzo[4,5:6,7]azuleno[1,8-*b,c*]fluorene **3a**, ^{1}H-NMR spectrum of this compound shows diastereotopic differentiation at CH_2 protons of the ethyl group with δ_H 4.55 (1 H, dq, J^2 14.4 Hz, J^3 7.19 Hz), 4.62 (1 H dq, J^2 14.5 Hz, J^3 7.26 Hz), a clear confirmation of the chiral vicinity (Figure 9). Compound **3a** shows absorption in UV-Vis spectrum at λ_{max} = 388 nm and emission at λ_{max} = 480 nm (Figure 10). Calculated UV-Vis spectrum shows absorption maxima at λ_{max} = 421 nm, and λ_{max} = 307 nm. Compound **3a** shows the lattice symmetry consistent with the Pbca space group in crystal. Two interactions are worth the brief description. Atoms N1 - C5, C14 - C16 and C29 - C34 forms approximately flat system of three aromatic rings which engaged in π–π contact with the same group of atoms, but related by inversion located at (0, 1/2, 0) in lattice. Note that unlike to compound **2a** this π–π interaction characterise much less effective overlapping. It also to be important in terms of crystal packing seems the contact (with distance 2.842 Å) of hydrogen atom at C36 to center phenyl ring formed by atom C7-C12. It complies with the condition of C-H – π interactions type III (Figure 11).

The racemat can be separated on two fractions with HPLC on OD-H chiral column with hexane-isopropanol eluent (Figure 12). CD spectrum of the less polar fraction (retention time 7.64 min.) shows weak positive Cottons effect with λ_{max} = 325 nm, and stronger negative at λ_{max} = 290 nm (Figure 13). Comparison of measured CD spectrum with calculated spectrum lead us to assess the chirality as (*M*) enantiomer, and the measured specific optical rotation $[\alpha]_D^{20}$ = +816º (± 131º) (CH_2Cl_2) gives finally configuration for this compound as *M*(+). Calculated specific optical rotation for enantiomer (*M*) $[\alpha]_D$ = + 205º. The second fraction from HPLC (retention time 10.1 min) shows opposite effects, week negative Cottons effect with λ_{max} = 325 nm, and stronger positive at λ_{max} = 290 nm (Figure 4 in Supp. Inf.). Comparison measured CD spectrum with calculated one lead us to assess the chirality as (*P*) enantiomer, and measured specific optical rotation $[\alpha]_D^{20}$ = -773º (± 187º) (CH_2Cl_2) gives finally configuration for this compound as *P*(-)-8-ethyl-6,8-dihydro-13-methyl-6-phenyl-5,6,7,8-tetraazadibenzo[4,5:6,7]azuleno[1,8-*bc*]fluorene. Comparison of the measured CD spectra for both fraction from chiral HPLC column shows exact opposite Cottons effects as expected for separated enantiomers of compound **3a** (Figure 14). Calculated racemisation barrier ΔG 6-31G(d) at 298.15 K to be 156 kJ/mol, and half-life time at 298.15 K is longer than 4 100 000 years, what exclude quick racemisation of **3a**. Fluorescence detected circular dichroism - FDCD spectrum of *M*(+) enantiomer of **3a** (fraction from HPLC with retention time 7.64 min.) indicate weak positive Cottons effect at 320 nm and strong negative at 290 nm (Figure 5 in Supp. Inf.). FDCD spectrum of **3a** *P*(-) enantiomer, the HPLC fraction with retention time of 10.1 min. shows weak negative Cottons effects at 320 nm and strong positive Cottons effect at 290 nm (Figure 6 in Supp.

Inf). Comparison of both enantiomers spectra of **3a,** *P*(-)and *M*(+) enantiomers shows mirror FDCD Cottons effects as expected for separated enantiomers (Figure 15).

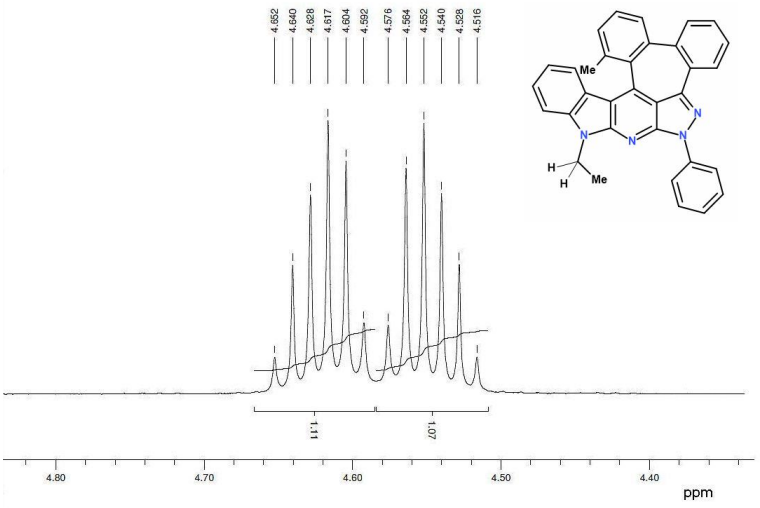

Figure 9. ^{1}H-NMR diastereotopic protons multiplets of methylene group, splitting of the ethyl moiety in asymmetric helical surroundings of **3a**. δ_H 4.55 (1 H, dq, J^{2} 14.4 Hz, J^{3} 7.19 Hz), 4.62 (1 H dq, J^{2} 14.5 Hz, J^{3} 7.26 Hz) Bruker 600 MHz, $CDCl_3$. Full spectrum – see Supp. Inf.

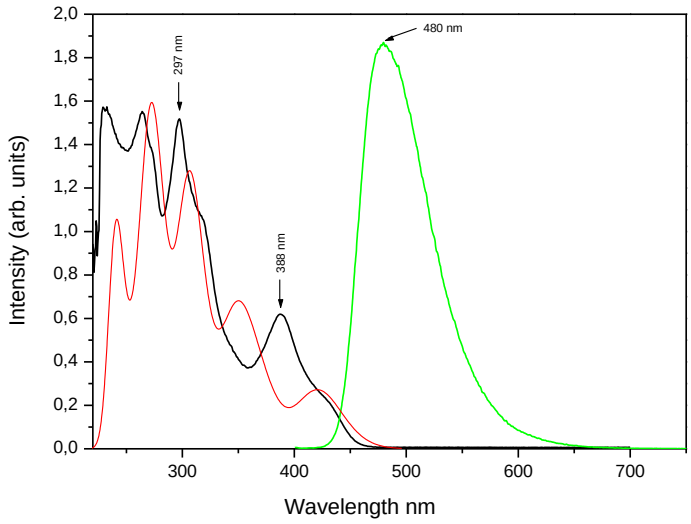

Figure 10. UV absorption (black line), calculated absorption spectrum (red line) and emission (green line) spectra of (*M*)(*P*)(±)-8-ethyl-6,8-dihydro-13-methyl-6-phenyl-5,6,7,8-tetraazadibenzo[4,5:6,7]-azuleno[1,8-*b*,*c*]fluorene **3a** in CH_2Cl_2. Excitation at 388 nm

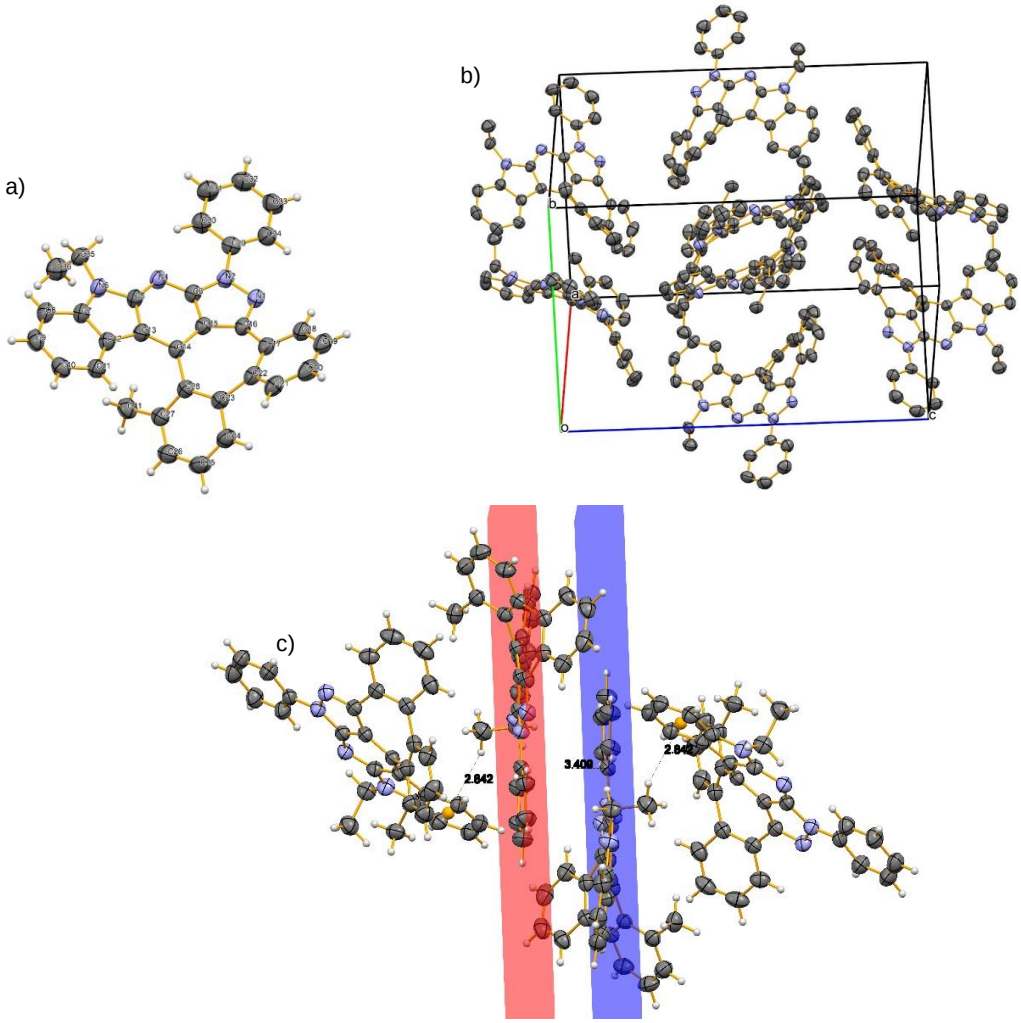

Figure 11. X-Ray structure of the compound **3a**: a) single molecule; b) crystal packing approximately towards [1 0 0] direction; c) π–π and C-H – π interactions

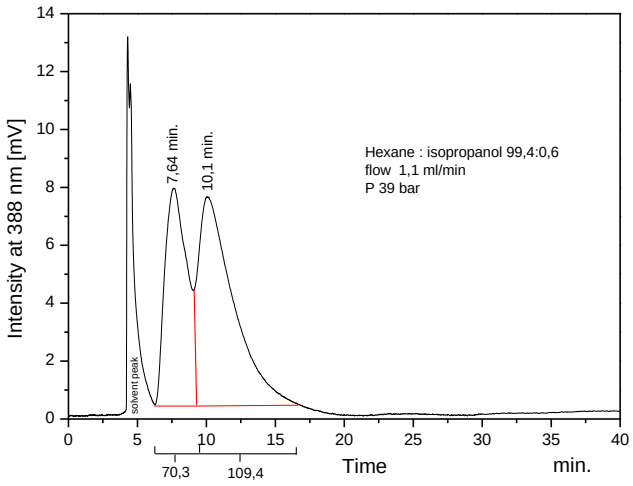

Figure 12. Separation of compound **3a** on to enantiomers on HPLC OD-H column with hexane-isopropanol eluent

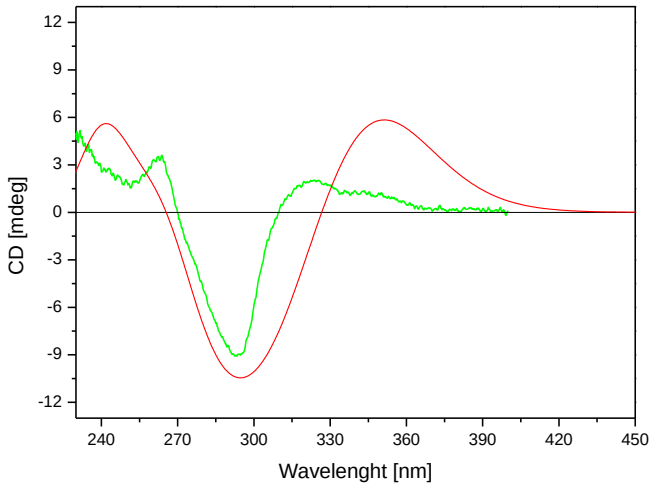

Figure 13. Measured CD spectrum of **3a** (fraction from HPLC with retention time 7.64 min) *M*(+)-8-ethyl-6,8-dihydro-13-methyl-6-phenyl-5,6,7,8-tetraazadibenzo[4,5:6,7]azuleno[1,8-*b*,*c*]fluorene, (green line, CH_2Cl_2) and calculated CD spectrum (red line), measured specific optical rotation $[\alpha]_D^{20}$ = +816º (± 131º) (CH_2Cl_2)

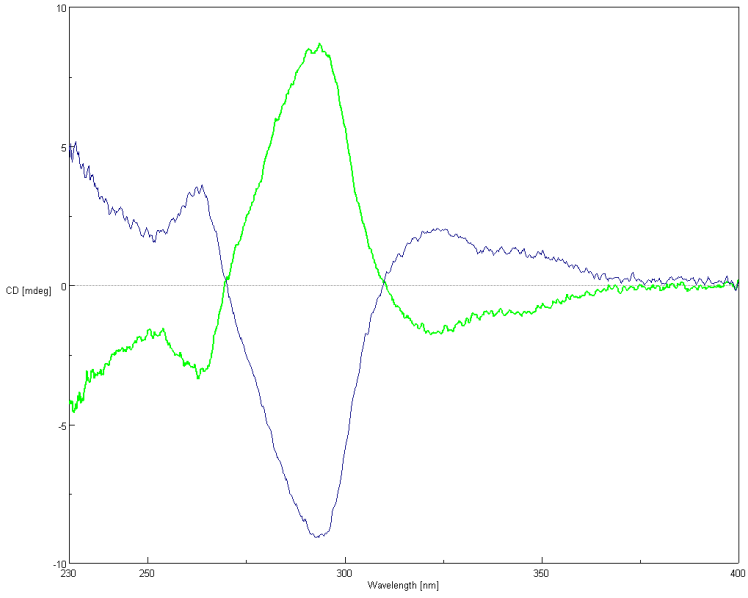

Figure 14. Comparison of the measured CD spectra for separated by HPLC fractions of **3a**. The first HPLC fraction 7.64 min (*M*)(+) enantiomer (blue line), and second fraction 10.1 min (green line) (*P*)(-) enantiomer (CH_2Cl_2)

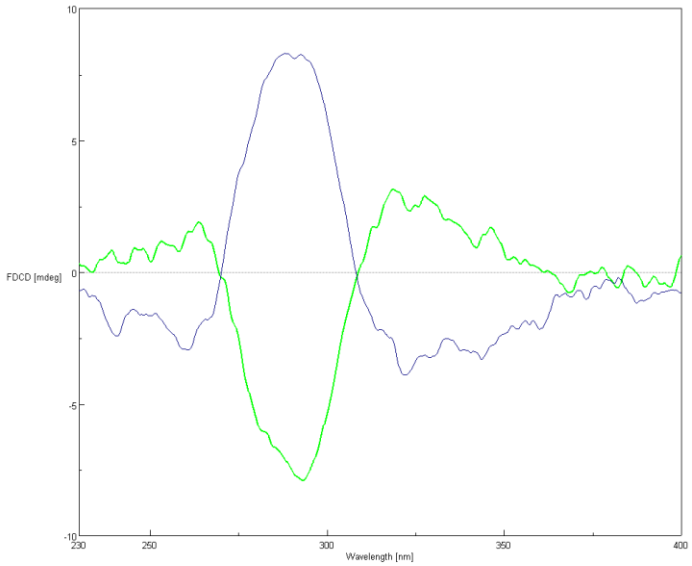

Figure 15. Comparison of the measured fluorescence detected circular dichroism (FDCD spectra) of **3a** enantiomers. **(*M*)(+)-3a** (green line) and **(*P*)(-)-3a** (blue line). (CH_2Cl_2) filter L-42

In compound **4a** we have enlarged the helically arranged rings with further benzo ring (Scheme 4).

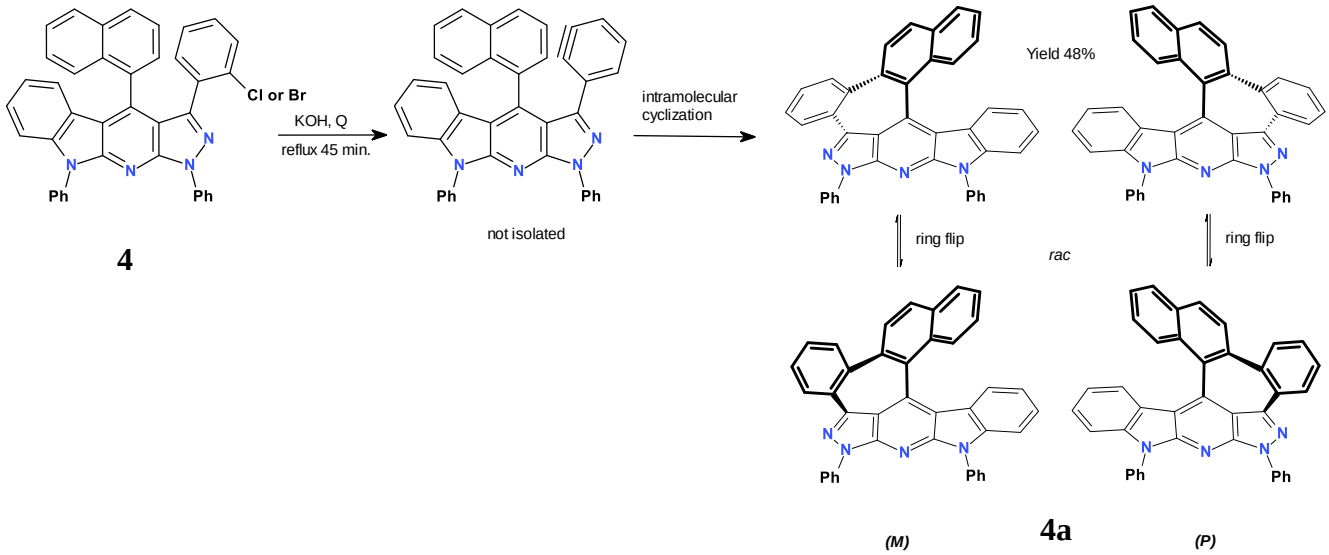

Scheme 4. Synthesis of **(***M***)(***P***)**(±)-6,8-dihydro-6,8-diphenyl-5,6,7,8-tetraaza-benzo[4,5]naphtho[2',1':6,7]azuleno[1,8-*b*,*c*]fluorene

(*M***)(***P***)**(±)-6,8-Dihydro-6,8-diphenyl-5,6,7,8-tetraazabenzo[4,5]naphtho[2',1':6,7]azuleno[1,8-*b*,*c*]fluorene **4a**, dark yellow solid, crystallize with cell symmetry consistent with the **P**-1 space group in triclinic crystal system. Unlike the previously discussed compounds **2a** and **3a** the asymmetric part of the unit cell contain both (*P*) and (*M*) enantiomers. It is worth noticing that although compounds **2a** and **4a** crystallize

in different types lattices, which shows completely different symmetry, their molecules forms locally very similar π–π complexes. For first molecule, of enantiomer (*P*), atoms N1 - C16 forms approximately flat system of four aromatic rings in central part of molecule, which is in π–π interaction, with their counterparts in molecule related by inversion located at (1/2, 1/2, 1/2), with 3.437 Å distance between planes. Similarly, atoms N51 - C66 in second molecule, of enantiomer (*M*), interacts with their analogue related by inversion at (1, 1/2, 0) and forms π–π complex, with 3.474 Å distance between planes. In both cases we have P...M and M...P dimers of enantiomers, respectively, because the molecules on π–π complexes are in the inversion relationship. Compound **4a** has no any methyl or methylene residues, so the C-H – π interactions are absent. It is also difficult to recognize other interaction with π electrons, but looking along direction [0 1 0], one can see how the molecules interlock to form a slider-like structure. It seems to be obvious that unclassified types of π–π interactions are present here.

The comparison of the crystal structures of the compounds for which they were determined *i.e.* **2a**, **3a** and **4a**, shows the obvious differences in the crystal packing and the symmetry of the lattice. They result from the presence of various substituents responsible for contacts with neighbouring molecules and minor differences in the geometry of the same molecule fragments for all three compounds. There are also some similarities. The most important of these is the tendency to form some kinds of dimers joined by π–π interactions. The molecules in these dimers are symmetric by inversion, so each dimer contain enantiomers P and M (Figure 16).

Compound **4a** possess absorption maxima in UV spectrum at λ_{max} = 395 nm and emission maxima at λ_{max} = 515 nm (Figure 17). Calculated UV-Vis spectrum shows absorption maxima at λ_{max} = 445 nm, and λ_{max} = 411 nm. The **4a** racemate can be separated with HPLC chiral column OD-H on two fraction (Figure 18), but those did not show optical rotation measured a few days after HPLC separation. We suppose that this compound exists in two conformational diastereoisomeric forms in an ratio near to 1:1. These diastereoisomeric forms arise probably from conformational 7-member ring flip, as shows on Scheme 4. Conformational ring flip is slow enough in NMR scale time to allow detection of both diastereoisomers, thus NMR spectra shows duplicate signals both in ^{1}H and ^{13}C spectres (see Figure 7 in Supp. Inf.). Similar behaviour in helicaly arranged rings involved also 7-member ring in propeller-shaped polycyclic aromatic hydrocarbon has been observed by Segawa, Itami *et al.*[10] In case of the compound **4a** the separation on HPLC leads possibly to a pair of enantiomers (*M*)(*P*) and (*M'*)(*P'*) which are not optically active as they are conformational diastereoisomers mixtures and still racemates. Calculated racemisation barrier ΔG 6-31G(d) at 298.15 K to be 141 kJ/mol, and half-life time at 298.15 K to be 7782 years, what rather excludes quick racemisation of **4a** enantiomers (CD measurements were performed a few weeks

after HPLC separation), astonishingly, the calculated racemisation barrier is notably lower than in compounds of **2a** and **3a**. Calculated specific optical rotation for enantiomer (*M*) $[\alpha]_D$ = + 30º suggests the (*M*)(+) and (*P*)(-) configurations for enantiomers of compound **4a**, however those possess additional chiral surface by meaning of side rings and shell be analysed as such with at least two surface chirality inclined evens, what additional complicated analyses (see Figure 8 and Movie 1 in Supp. Inf.).

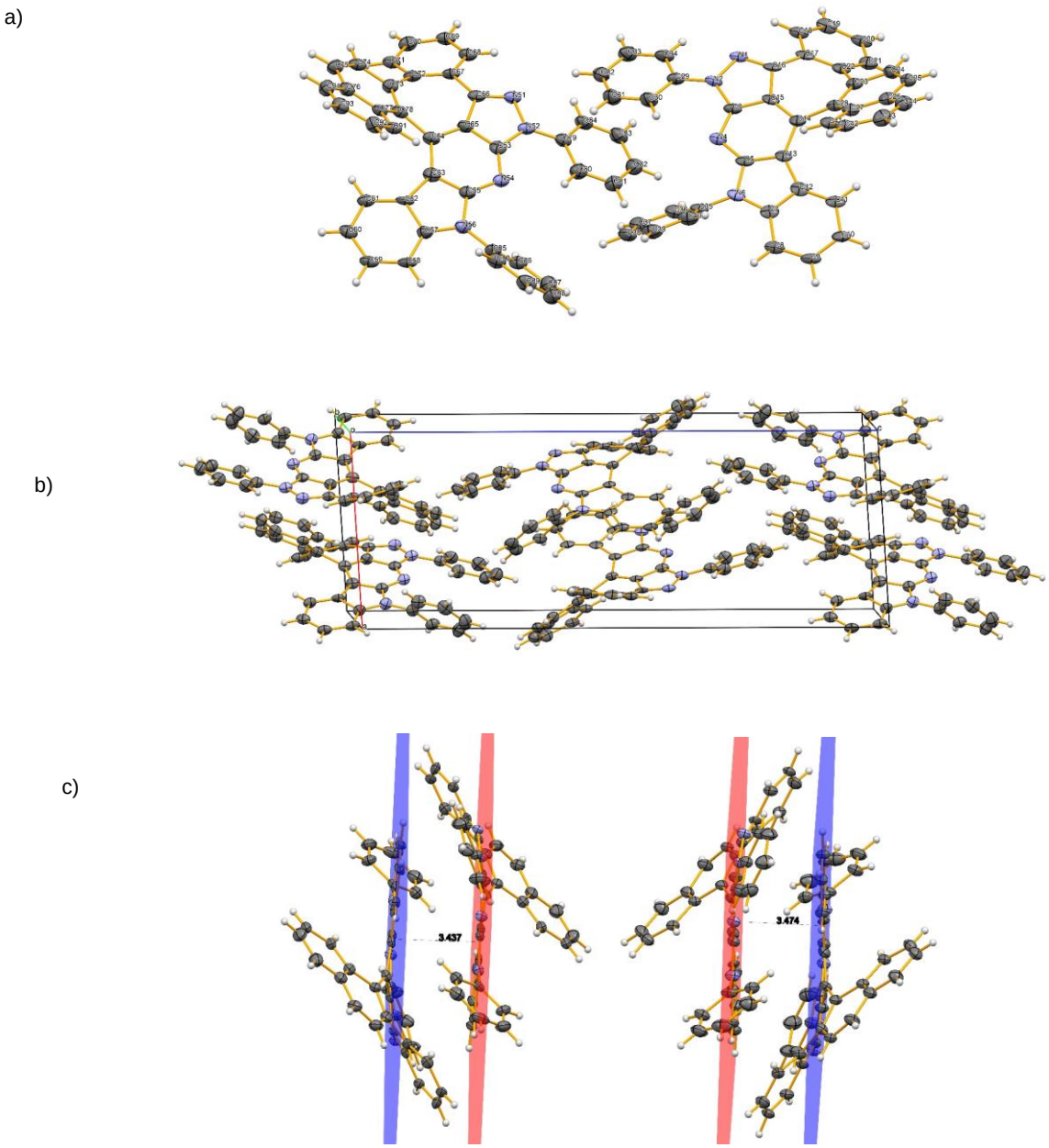

Figure 16. X-Ray structure of the compound **4a**: a) asymmetric unit containing enantiomers (*P*) and (*M*), with labels; b) crystal packing towards [0 1 0] direction; c) π–complexes of **4a** compound, complexes were separated for clarity

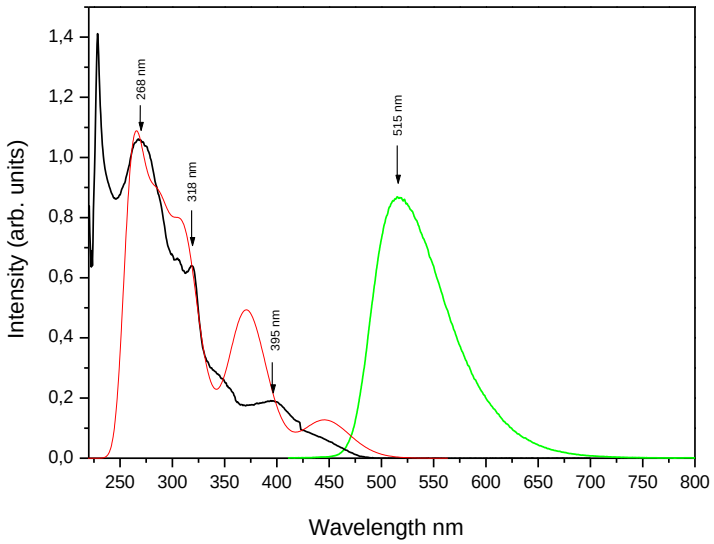

Figure 17. UV absorption (black line – measured spectrum, red line – calculated spectrum) and emission spectrum (green line) of **4a** in CH_2Cl_2. Excitation at 395 nm

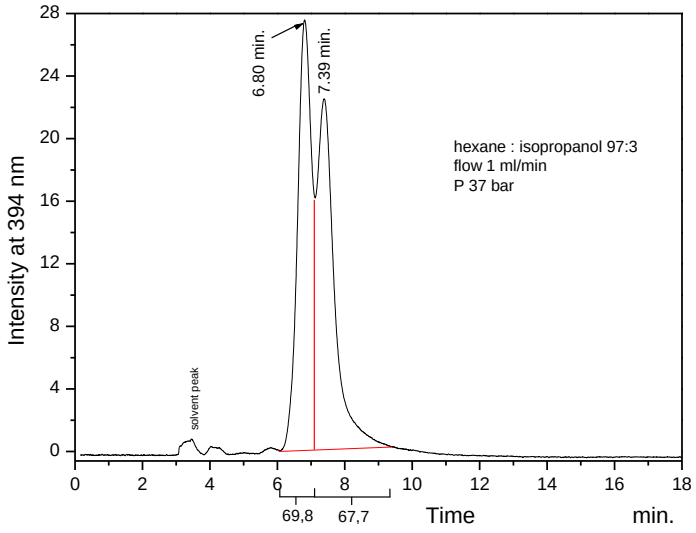

Figure 18. Separation of **4a** on HPLC OD-H column on two fraction with hexane-isopropanol eluent

In compound **5a** we have annulated the helically arranged rings with further benzo ring at the opposite side of helical surface.

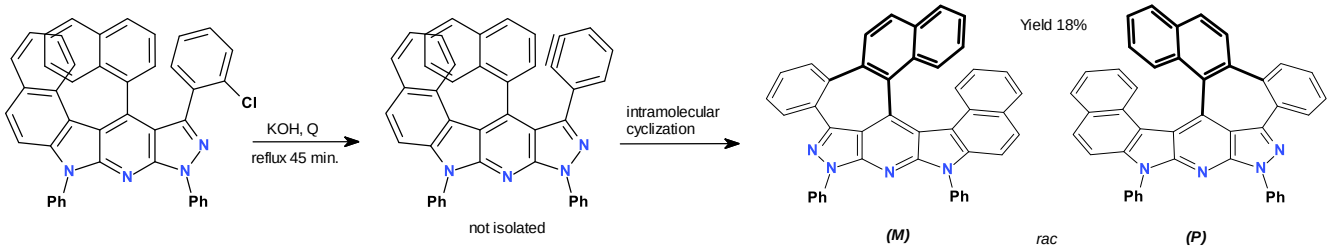

5 **5a**

Scheme 5. Synthesis of **5a** (*M*)(*P*)(±)-6,8-dihydro-6,8-diphenyl-5,6,7,8-tetra-azabenzo[*g*]benzo[6,5]naphtho[2',1':6,7]azuleno[1,8-*b*,*c*]fluorene

(*M*)(*P*)(±)-6,8-Dihydro-6,8-diphenyl-5,6,7,8-tetraazabenzo[*g*]benzo[6,5]naphtho[2',1':6,7]azuleno[1,8-*b*, *c*]fluorene **5a** - isolated as orange solid, with absorption maxima at λ_{max} = 401 nm and λ_{max} = 319 nm, and emission at λ_{max} = 519 nm (Figure 19). Calculated UV-Vis spectrum shows absorption maxima at λ_{max} = 470 nm, and λ_{max} = 379 nm, and λ_{max} = 327 nm. The attempt to separate compound **5a** on to enantiomers failed. Unfortunately we were not able to find the conditions for HPLC separation of **5a** racemate to enantiomers, neither with OD-H column nor with other columns like AS-H and OJ-H. Calculated racemisation barrier ΔG 6-31G(d) is 193 kJ/mol at 298.15 K, and the half-life time at 298.15 K is 1.35×10^{13} years, what excludes racemisation of **5a** enantiomers.

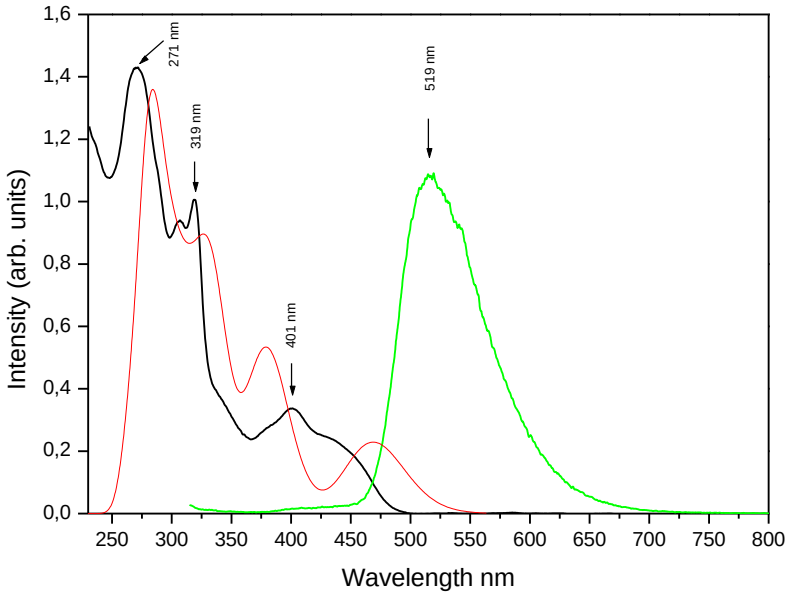

Figure 19. UV absorption (black line), calculated absorption spectrum (red line) and, emission spectrum (green line) of **5a** in CH_2Cl_2. Excitation at 271 nm

Table 1. Substituted 5,6,7,8-tetraaza-azuleno[1,8-*b*,*c*]fluorenes synthesis and properties

Substrate	Reaction time [min.]	Product	Yield (%)	Mp ºC	λ_{abs} [nm]	λ_{fl} [nm]
1	30	**1a**	73	319-321 $CHCl_3$/MeOH	389	482
2	30	**2a**	49	270-274 CH_2Cl_2/MeOH	388	479
3	30	**3a**	46	265-269 toluene/MeOH	388	480
4	45	**4a**	48	278-282 CH_2Cl_2/acetone	394	515
5	60	**5a**	18	303-306 CH_2Cl_2/acetone	401	519

CONCLUSIONS

Reaction. The reaction conditions are very harsh (melted KOH, quinoline reflux, ca. 237 ºC), and reaction time increase with increasing of the steric hindrance in the substrate. The yields decrease with longer reaction time because decomposition reactions occur. Increased yields were reached if higher dilution and heating attenuation were applied. Palladium catalysed cyclization the bromo analogues compounds **1-5** to **1a-5a** can be performed in DMF at 140 ºC, however the reaction time over 24 hours is necessary, and the yields are not much higher as in quinoline reflux. We have also attempt to synthesised homologs to compounds **1-5** possessing electrondonor substituents at the benzo rings side, but the three component reaction described by Bazgir *et al.*[8] used for synthesis of the starting compounds does not work well in this case, so we isolated only traces of the products.

Photoluminescence. All studied substituted 5,6,7,8-tetraaza-azuleno[1,8-*b*,*c*]fluorenes show intense yellow-green luminescence in solution and in steady state, a prerequisite to be the candidate in OLED technology. Additionally, the robust to high temperature and high racemisation barrier are another requirement to make some of these compounds amenable in OLEDs with circularly polarised luminescence. The shift of the photoluminescence maxima from λ_{max} = 479 nm for **2a** to λ_{max} = 519 nm for **5a** resulted of the bathochromic effect of the additional benzene rings in chromophore (Table 1, Figure 20). The photoluminescence maxima wavelength were independent of the excitation wavelength.

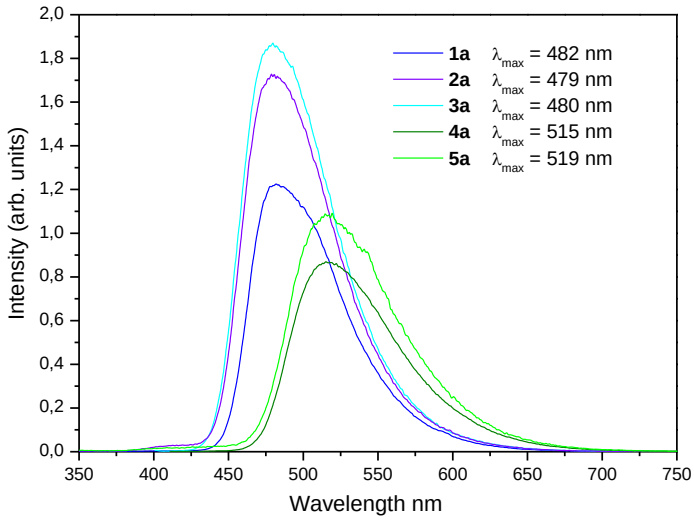

Figure 20. Comparison of the UV emission spectra of substituted 5,6,7,8-tetraaza-azuleno[1,8-*b*,*c*]fluorenes **1a-5a** in CH_2Cl_2 (different concentrations)

EXPERIMENTAL

*Substituted 5,6,7,8-tetraaza-azuleno[1,8-b,c]fluorenes **1a-5a** synthesis, a general procedure*. In quartz glass vessel the precursor of tetraza-azulenofluorene (**1-5**) was dissolved in dry, freshly distilled quinoline, powdered KOH was added in 4 fold excess. Then the mixture was refluxed under nitrogen for 15-60 min depending on the substrate (Table 1). The conversion of the substrate to product was monitored in UV light, by changes of the solutions colour from blue to yellow-green. The reaction was cooled to rt, washed with water, treated with 4M HCl and extracted with toluene. The organic layer was washed with 5% aqueous $NaHCO_3$ and dried (Na_2SO_4). The solvent was removed *in vacuo* and residue was crystallized from CH_2Cl_2/MeOH, CH_2Cl_2/acetone or toluene/MeOH, alternatively it was purified by column chromatography on Al_2O_3 with toluene-hexane eluent. Supporting information with furthermore experimental details for this article is given.

FOUNDING

This work was supported by the Ministry of Science and Higher Education, Warsaw, Poland [grant 6903/IA/SP/2018].

ACKNOWLEDGEMENTS

We thank Prof. Dr Dariusz Cież for helpful discussion and CD-spectra measurement.

REFERENCES

1. a) G. Albano, G. Pescitelli, and L. Di Bari, *Chem. Rev.*, 2020, **120**, 10145; b) G. Longhi, E. Castiglioni, J. Koshoubu, G. Mazzeo, and S. Abbate, *Chirality*, 2016, **28**, 696; c) K. Soai, T. Kawasaki, and A. Matsumoto, *Tetrahedron*, 2018, **74**, 1973; d) E. M. Sanchez-Carnerero, A. R. Agarrabeitia, F. Moreno, B. L. Maroto, G. Muller, M. J. Ortiz, and S. de la Moya, *Chem. Eur. J.*, 2015, **21**, 13488; e) M. Weimar, R. Correa da Costa, F.-H. Lee, and M. J. Fuchter, *Org. Lett.*, 2013, **15**, 1706; f) T. Otani, A. Tsuyuki, T. Iwachi, S. Someya, K. Tateno, H. Kawai, T. Saito, K. S. Kanyiva, and T. Shibata, *Angew. Chem. Int. Ed.*, 2017, **56**, 3906; g) J. Bailey, A. Chrysostomou, J. H. Hough, T. M. Gledhill, A. McCall, S. Clark, F. Menard, and M. Tamura, *Science*, 1998, **281**, 672.
2. Y. Yang, R. Correa da Costa, D. M. Smilgies, A. J. Campbell, and M. J. Fuchter, *Adv. Mater.*, 2013, **25**, 2624.
3. B. Doistau, J.-R. Jiménez, and C. Piguet, *Front. Chem.*, 2020, **8**, art. 555.
4. a) N. Chen and B. Yan, *Molecules*, 2018, **23**, 3376; b) Y. Morisaki and Y. Chujo, *Bull. Chem. Soc. Jpn.*, 2019, **92**, 265; c) K. Goto, R. Yamaguchi, S. Hiroto, H. Ueno, T. Kawai, and H. Shinokubo, *Angew. Chem. Int. Ed.*, 2012, **51**, 10333; d) K. Usui, K. Yamamoto, T. Shimizu, M. Okazumi, B. Mei, Y. Demizu, M. Kurihara, and H. Suemune, *J. Org. Chem.*, 2015, **80**, 6502.
5. a) P. Szlachcic, K. S. Danel, M. Gryl, K. Stadnicka, Z. Usatenko, N. Nosidlak, G. Lewinska, J. Sanetra, and W. Kuznik, *Dyes Pigm.*, 2015, **114**, 184; b) S. Calus, K. S. Danel, T. Uchacz, and A.V. Kityk, *Mater. Chem. Phys.*, 2010, **121**, 477; c) K. S. Danel, T. Uchacz, and M. Karelus, *ARKIVOC*, 2011, **ix**, 272; d) P. Gąsiorski, K. S. Danel, M. Matusiewicz, T. Uchacz, and A. V. Kityk, *Dyes Pigm.*, 2012, **93**, 1538; e) K. S. Danel, A. Wisła, and T. Uchacz, *ARKIVOC*, 2009, **x**, 71.
6. K. S. Danel, G. Lewińska, Z. Usatenko, T. Lemek, and A. Wisła-Świder, *J. Phys. Conf. Ser.*, 2019, **1186**, 012012.
7. K. Danel and T. Uchacz, *Intertech Proceedings*, 2011, 268.
8. a) R. Ghahremanzadeh, S. Ahadi, and A. Bazgir, *Tetrahedron Lett.*, 2009, **50**, 7379; b) H. Yupeng, Q. Wei, G. Dewen, and T. Yao, Wuhan Shengchengyu Tech. LLC., PRC, Faming Zhuanli Shenqing Patent, 2018, CN 109096281, A.
9. J. F. Malone, C. M. Murray, M. H. Charlton, R. Docherty, and A. J. Lavery, *J. Chem. Soc., Faraday Trans.*, 1997, **93**, 3429. See also C. A. Hunter and J. K. M. Sanders, *J. Am. Chem. Soc.*, 1990, **112**, 5525.
10. K. Kawai, K. Kato, L. Peng, Y. Segawa, L. T. Scott, and K. Itami, *Org. Lett.*, 2018, **20**, 1932.